 doi:10.20944/preprints202204.0244.v1

Article

A Fuzzy Consensus Clustering Algorithm for MRI Brain Tissue Segmentation

S V Aruna Kumar [1]*, Ehsan Yaghoubi [2] and Hugo Proença [3]*

[1] Department of Computer Science and Engineering, Malnad College of Engineering, Hassan, Karnataka; arunkumarsv55@gmail.com
[2] Department of Informatics, University of Hamburg, Hamburg, Germany; ehsan.yaghoubi@uni-hamburg.de
[3] Department of Computer Science, University of Beira Interior, Portugal; hugomcp@di.ubi.pt
* Correspondence: arunkumarsv55@gmail.com;hugomcp@di.ubi.pt

Abstract: Brain tissue segmentation is an important component of clinical diagnosis of brain diseases by means of multi-modal magnetic resonance imaging (MR). Brain tissue segmentation is developed by many unsupervised methods in literature. The most commonly used unsupervised methods are: K-Means, Expectation Maximization and Fuzzy Clustering. Fuzzy clustering methods offer considerable benefits compared with the aforementioned methods as they are capable of handling brain images which are complex, largely uncertain and imprecise in nature. However, this approach suffers from the intrinsic noise and intensity inhomogeneity (IIH) in the data resulted from the acquisition process. To resolve these issues, we propose a fuzzy consensus clustering algorithm that defines a membership function resulted from a voting schema to cluster the pixels. In particular, we first pre-process the MRI data and employ several segmentation techniques based on traditional fuzzy sets and intuitionistic sets. Then, we adopted a voting schema to fuse the results of the applied clustering methods. Finally, to evaluate the proposed method, we used the well-known performance measures (boundary measure, overlap measure and volume measure) on two publicly available datasets (OASIS and IBSR18). The experimental results show the superior performance of the proposed method in comparison with the recent state of the arts.

Keywords: Brain Tissue Segmentation; Consensus Clustering; Segmentation; Magnetic Resonance Image

1. Introduction

Segmenting brain tissue is the process of subdividing the image of the brain into major components like Cerebrospinal Fluid (CSF), Gray Matter (GM) and White Matter (WM). The step of brain tissue segmentation is fundamental in diagnosing and monitoring a wide range of neurological diseases. Several researchers have strived to develop automatic brain tissue segmentation in the last two decades [1].

Brain tissue segmentation is developed by many unsupervised methods in literature. The most commonly used unsupervised methods are: K-Means [2–4], Expectation Maximization [5] and Fuzzy Clustering [6,7]. Fuzzy clustering methods offer considerable benefits compared with the aforementioned methods as they are capable of handling brain images which are complex, largely uncertain and imprecise in nature.

Even though, traditional Fuzzy C-Means (FCM) showcased outstanding results on brain image segmentation, it has some limitation such as being sensitive to noise due to the use of euclidean distance metric and neighbourhood information ignorance. The FCM computes the distance between cluster center and voxels using euclidean distance measure. Euclidean distance is very sensitive to noise which results in deterioration of segmentation results. From the literature, we found many variants of FCM methods which are developed to address the aforementioned shortcomings. To address the noise sensitivity, researchers added the spatial information into FCM objective function [8,9]. The addition of spatial function to objective function helps to reduce the impact of noise and also it helps to enhance the performance. The spatial information may be local or global [10]. On the other hand, to address the limitations of Euclidean distance, many researchers developed

Citation: Aruna Kumar, S V.; Yaghoubi, Ehsan.;Proença , Hugo. Title. *Preprints* **2022**, *1*, 0. https://doi.org/

 doi:10.20944/preprints202204.0244.v1

kernel version of FCM and named it as Kernel FCM (KFCM) [11,12]. KFCM adopts kernel function as a distance measure. The kernel function transfers the input data to higher dimensional kernel space and makes clustering task easier.

The aforementioned FCM variant methods are based on traditional fuzzy set. In fuzzy set, non membership value is always the complement of membership value. However, in real time this assumption fails due to hesitation. The hesitation arises due to uncertainty in defining membership function. To handle this hesitation, Atanassov [13] developed a advanced fuzzy set called Intutionistic Fuzzy Set (IFS). In IFS, the non membership value is computed using the fuzzy complement generator functions. In recent times, researchers have given more attention in developing IFS based clustering methods [14–17]. Chaira [15] developed an Intuitionistic Fuzzy C-Means (IFCM) where the intuitionistic fuzzy entropy is added to conventional FCM objective function. The intuitionistic fuzzy set handles the uncertainty which originates while defining a membership function by considering the hesitation degree. To handle noise and uncertainty during segmentation, Verma et al., [18] considered both the pixel and local neighbourhood information. The main benefit of this method is that it is non parametric.

Recently, researchers come to realize that a single clustering method might fail to produce good results with complex data. Hence, they are concentrating on developing consensus clustering methods [19,20]. Consensus clustering is also known as cluster ensemble and its main aim is to find a single partition of data with overlapping clusters. In literature, it has been widely agreed that consensus clustering can generate robust results [21–24]. Motivated by the advantages of consensus clustering, in this paper we are proposing a brain tissue segmentation method based on consensus clustering. The proposed method consist of two steps: Pre-processing and Segmentation. In pre-processing, the brain images are pre-processed by employing registration, skull stripping, bias field correction. In the segmentation step, initially, the brain images are segmented using four different clustering methods. The two clustering methods are based on traditional fuzzy set and other two are based on Intutionistic set. In traditional fuzzy set category, Robust Spatial Kernel FCM (RSKFCM) [25] and Generalized Spatial Kernel FCM (GSKFCM) [26] are employed. On the other hand, in intuitionistic fuzzy set category, two variants of Modified Intuitionistic Fuzzy C-Means [17] are employed. Further, the results of four individual clustering methods are combined using voting schema. The proposed approach is evaluated on two MRI publicly available datasets: OASIS and IBSR18 Dataset and the results are compared using the results with state-of-art methods

The remainder of the paper is as follows: section 2 presents the methodology of proposed method. We then introduced the datasets and the evaluation metrics along side the implementation details and discussions on the performance of the proposed method in section 3. Finally conclusion of the paper is presented in section 4.

2. Methodology

2.1. Pre-processing

We perform three pre-processing steps namely Registration, Bias Field correction and Skull Stripping. Registration is the process of spatially aligning two or more images of the same content, taken from a different view and/or at a different time and is required to align the multi-modal image of the same patient. Bias Field refers to a low frequency signal which corrupts the MRI images due to inhomogeneities in the magnetic field of the MRI machines. Bias field leads to intensity inhomogeneity and in turn it affects the segmentation accuracy. Hence, bias field need to be corrected before doing the segmentation. Skull Stripping is the process of removing non brain tissues such as fat, skull and neck. These non brain tissues have an intensity that overlaps with the intensity of the other brain tissues. Thus, the brain tissues have to be extracted before the brain segmentation. There are many skull stripping methods such as Brain Extraction Tool (BET) [27], Brain Surface Extraction (BSE)

 doi:10.20944/preprints202204.0244.v1

[28], AFNI [1], BridgeBurner [29], GCUT [30] and ROBEX [31]. Among all these methods, ROBEX provides significantly improved performance [31].

All the aforementioned steps are optional and depend on the image data used for the study. Hence, in this paper, different pre-processing steps are performed for different datasets. The pre-processed brain images are segmented using consensus clustering. The following subsection presents a detailed description regarding segmentation.

2.2. Segmentation

The proposed consensus clustering method consists of a combination of traditional fuzzy sets and Intutionistic sets to not only increase the robustness to the noise but also use the neighborhood information when forming the clusters. To do so, we use the Robust Spatial Kernel FCM (RSKFCM) [25] and Generalized Spatial Kernel FCM (GSKFCM) [26] methods along side the two variants of the Modified Intuitionistic Fuzzy C-Means [17] technique. Finally, we fuse the results of the clustering methods using voting schema. Next subsections explain the employed clustering methods and the voting schema in detail.

2.2.1. Robust Spatial Kernel FCM (RSKFCM)

Robust Spatial Kernel Fuzzy C-Means (RSKFCM) [25] is the variant of conventional Fuzzy C-Means (FCM). RSKFCM addresses the noise sensitivity and neighborhood information ignorance limitations of FCM. RSKFCM injects the neighbourhood information into the FCM objective function and uses the Gaussian Kernel function instead of euclidean metric.
The main aim of the RSKFCM is to minimize the objective function shown in equation 1

$$J = \sum_{i=1}^{c} \sum_{j=1}^{n} w_{ij}^{m} \ \|\Phi(x_j) - \Phi(v_i)\|^2 \tag{1}$$

Where c is the number of clusters, n is the number of voxels, m is a fuzzifier value, which controls the fuzziness of the resulting partition, w_{ij} is the RSKFCM membership degree of x_j in i^{th} cluster. v_i is the ith cluster center, Φ is an implicit non linear map which is computed as:

$$\|\Phi(x_j) - \Phi(v_i)\|^2 = K(x_j, x_j) + K(v_j, v_j) - 2K(x_j, v_i) \tag{2}$$

where K is the inner product of kernel function i.e., $K(x, y) = \Phi(x)^T \Phi(y)$. In this paper, we have adopted the Gaussian kernel function which is defined as:

$$K(x, y) = \exp\left(-\|x - y\|^2 \Big/ \sigma^2\right) \tag{3}$$

In Gaussian kernel $K(x, x) = 1$ and $K(v, v) = 1$, hence the kernel function becomes:

$$\|\Phi(x_j) - \Phi(v_i)\|^2 = 2(1 - K(x_j, v_i)) \tag{4}$$

Substituting equation 4 in equation 1, the objective function becomes:

$$J = 2 \sum_{i=1}^{c} \sum_{j=1}^{n} w_{ij}^{m} \ (1 - K(x_j, v_i)) \tag{5}$$

[1] "Analysis of Functional NeuroImages" (AFNI) software package publicly available at https://afni.nimh.nih.gov/.

Preprints (www.preprints.org) | NOT PEER-REVIEWED | Posted: 26 April 2022 doi:10.20944/preprints202204.0244.v1

RSKFCM membership function w_{ij} is the combination of kernel membership function u_{ij} and neighbourhood function s_{ij} and it is computed as.

$$w_{ij} = \frac{u_{ij}^{p} s_{ij}^{q}}{\sum_{k=1}^{c} u_{kj}^{p} s_{kj}^{q}} \tag{6}$$

where p and q are parameter to control the relative importance of kernel membership and neighbourhood membership functions.
The kernel and neighbourhood membership functions are computed using equation 7 and 8

$$u_{ij} = \frac{\left(1 - K(x_j, v_i)\right)^{-1/(m-1)}}{\sum_{k=1}^{c} \left(1 - K(x_j, v_k)\right)^{-1/(m-1)}}; \tag{7}$$

$$s_{ij} = \sum_{k \in N_k(x_j)} u_{ik} \tag{8}$$

where $N_k(x_j)$ represents neighbourhood voxels of x_j. This neighbourhood function represents the probability that the voxel x_j belongs to i^{th} cluster.
Similar to FCM, RSKFCM also works in an iterative process to update the membership and cluster center values. The cluster centers are updated using equation 9

$$v_i = \frac{\sum_{j=1}^{n} w_{ij}^{m} K(x_j, v_i) x_j}{\sum_{j=1}^{n} w_{ij}^{m} K(x_j, v_i)} \tag{9}$$

RSKFCM is an iterative process and it stops when the stopping criteria is satisfied i.e., the difference of successive iteration's objective function value is less than the user specified stopping criteria value.

2.2.2. Generalized Spatial Kernel FCM (GSKFCM)

Generalized Spatial Kernel FCM (GSKFCM)[26] is also a another variant of conventional FCM. Even though, RSKFCM overcomes the limitations of FCM, the performance is not good due to (i) it injects neighborhood information only into objective function. However, distance function plays a vital role in computing the membership value. Thus addition of neighborhood information can increase the performance. and (ii) it assumes all features have equal importance. However, in real world problem all the features may not be equally important. GSKFCM overcomes these aforementioned limitations by injecting the weighted neighbourhood information into distance function and employing the Gaussian kernel as the distance metric.
The aim of the GSKFCM is to minimize the objective function shown in equation 10.

$$J = 2 \sum_{i=1}^{c} \sum_{j=1}^{n} z_{ij}^{m} d_{new}^{2}(x_j, v_i) \tag{10}$$

where z_{ij} is the GSKFCM membership function and it is computed as:

$$z_{ij} = \frac{1}{\sum_{k=1}^{c} \left(\frac{d_{new}^{2}(x_j, v_i)}{d_{new}^{2}(x_j, v_k)} \right)^{\frac{1}{(m-1)}}} \tag{11}$$

Preprints (www.preprints.org) | NOT PEER-REVIEWED | Posted: 26 April 2022 doi:10.20944/preprints202204.0244.v1

Where d_{new} is the GSKFCM distance function which incorporates the neighbourhood function into distance function and it is computed as:

$$d^2_{new}(x_j, v_i) = d^2(x_j, v_i)\ f(p_{ij}) \tag{12}$$

where, $d^2(x_j, v_i)$ is the Gaussian Kernel distance function shown in equation 4 and $f(p_{ij}) = \frac{1}{p_{ij}}$ is the neighbourhood function.

GSKFCM considers the neighbourhood information and computes the membership value associated with each voxel as weighted sum of traditional FCM membership value and the membership value of the N_k neighbour points. The neighbourhood function (p_{ij}) is defined as:

$$p_{ij} = \sum_{k=0}^{N_k} h(x_j, x_k) g(u_{ik}) \tag{13}$$

Where N_k is the number of neighbourhood voxels, $g(u_{ik}) = u_{ik}$ is the membership function (equation 7), $h(x_j, x_k)$ is the distance function which is computed as:

$$h(x_j, x_k) = \left(\sum_{l=0}^{N_k} \frac{d^2(x_j, x_k)}{d^2(x_j, x_l)} \right)^{-1} \tag{14}$$

Substituting equation 14 in 13, the neighbourhood function becomes:

$$p_{ij} = \sum_{k=0}^{N_k} g(u_{ik}) \left(\sum_{l=0}^{N_k} \frac{d^2(x_j, x_k)}{d^2(x_j, x_l)} \right)^{-1} \tag{15}$$

Substituting equation 12 in equation 11, the membership function z_{ij} becomes,

$$z_{ij} = \left(\sum_{k=1}^{c} \left(\frac{d^2(x_j, v_i)\ f(p_{ij})}{d^2(x_j, v_k)\ f\left(p_{jk}\right)} \right)^{\frac{1}{(m-1)}} \right)^{-1} \tag{16}$$

$$= \frac{\left(\sum_{k=1}^{c} \left(\frac{d^2(x_j, v_i)}{d^2(x_j, v_k)} \right)^{\frac{1}{m-1}} \right)^{-1} f^{\frac{1}{1-m}}(p_{ij})}{\sum_{k=1}^{c} \left(\sum_{l=1}^{c} \left(\frac{d^2(x_j, v_i)}{d^2(x_j, v_l)} \right)^{\frac{1}{m-1}} \right)^{-1} f^{\frac{1}{1-m}}\left(p_{jk}\right)} \tag{17}$$

where $\left(\sum_{k=1}^{c} \left(\frac{d^2(x_j, v_i)}{d^2(x_j, v_k)} \right)^{\frac{1}{m-1}} \right)^{-1} = u_{ij}$. Then the membership function z_{ij} becomes

$$z_{ij} = \frac{u_{ij} f^{\frac{1}{1-m}}(p_{ij})}{\sum_{k=1}^{c} u_{jk} f^{\frac{1}{1-m}}\left(p_{jk}\right)} \tag{18}$$

Similar to FCM and RSKFCM, GSKFCM operates as an iterative process by updating membership and cluster center value. The cluster centers are updated using equation 19

$$v_i = \frac{\sum_{j=1}^{n} z_{ij}^m K(x_j, v_i) x_j}{\sum_{j=1}^{n} z_{ij}^m K(x_j, v_i)} \tag{19}$$

Preprints (www.preprints.org) | NOT PEER-REVIEWED | Posted: 26 April 2022 doi:10.20944/preprints202204.0244.v1

GSKFCM decides the label based on the maximum membership value.

2.2.3. Modified Intuitionistic Fuzzy C-Means (MIFCM)

Modified Intuitionistic Fuzzy C-Means (MIFCM) [17] is the variant of the conventional Intuitionistic Fuzzy C-Means (IFCM) [15] and it is based on intuitionistic fuzzy set. In MIFCM, the input data is clustered by optimizing the following objective function shown in equation 20

$$J = \sum_{j=1}^{n} \sum_{i=1}^{c} \beta_{ij}^{m} \, d_H(x_j, v_i) \tag{20}$$

where, x_j represents j^{th} voxel, v_i refers to i^{th} cluster center, m refers to the fuzzification value, β_{ij} refers to the MIFCM membership value of j^{th} voxel to i^{th} cluster, $d_H(x_j, v_i)$ is the modified Hausdorff distance between j^{th} voxel to i^{th} cluster center.
Similar to Fuzzy C-Means, MIFCM optimizes the objective function iteratively by updating the membership and cluster centers. The MIFCM membership value is updated using equation

$$\beta_{ij} = \mu_{ij} + \pi_{ij} \tag{21}$$

where μ_{ij} is membership value and π_{ij} is hesitation value. The membership value μ_{ij} is computed as follows: 22

$$\mu_{ij} = \frac{1}{\sum_{k=1}^{c} \left(\frac{d_H(x_j, v_i)}{d_H(x_j, v_k)} \right)^{\frac{2}{m-1}}} \tag{22}$$

The hesitation value π_{ij} is the combination of membership and non membership value and it is computed as:

$$\pi_{ij} = 1 - \mu_{ij} - \eta_{ij} \tag{23}$$

where η_{ij} is the non membership value. To compute non membership value, Sugeno's and Yager's intuitionistic fuzzy complement generators are used and which are computed using equations 24 and 25 respectively.

$$\eta_{ij} = \frac{1 - \mu_{ij}}{1 + \alpha \mu_{ij}} \tag{24}$$

$$\eta_{ij} = (1 - (\mu_{ij})^{\alpha})^{\frac{1}{\alpha}} \tag{25}$$

where $\alpha > 0$ is constant.
In this paper, we employed both Sugeno's and Yager's complement generators. MIFCM using sugeno's function is named as MIFCM_S and similarly MIFCM using Yager's function is named as MIFCM_Y. Further, cluster centers are updated using equations 26.

$$v_i = \frac{\sum_{j=1}^{n} \beta_{ij}^{m} x_j}{\sum_{j=1}^{n} \beta_{ij}^{m}} \tag{26}$$

MIFCM is an iterative process and it stops when the convergence criteria is satisfied (i.e., the difference between objective function value of successive iterations is less than the user specified stopping criteria value).

2.2.4. Voting Schema

In this section, the segmentation results are combined using voting schema. Let U_1, U_2, U_3 and U_4 presents the membership matrix of RSKFCM, GSKFCM, MIFCM_S and MIFCM_Y respectively. From these membership matrices, label for each pixel is computed. The pixel x_j is assigned a label of a cluster for which it has maximum membership value.

Preprints (www.preprints.org) | NOT PEER-REVIEWED | Posted: 26 April 2022 doi:10.20944/preprints202204.0244.v1

Let P_1, P_2, P_3 and P_4 is the label matrix created for RSKFCM, GSKFCM, MIFCM_S and MIFCM_Y respectively. From these label matrices, consensus results are produced using voting method. The pixel x_j is assigned to a cluster based on maximum number of cluster label i.e $label = argmax_i\left(P^{(i)}_{(l)}\right)$, where $l = \{1,2,3,4\}$ and $1 \leq i \leq c$.

3. Experimental Results

This section presents, the dataset used for experimentation, metrics used to evaluate the proposed method, experimental setup followed by result and discussion.

3.1. Datasets

To asses the proposed method, we carried out experiments on two publicly available standard datasets.

3.1.1. OASIS

The Open Access Series of Imaging Studies (OASIS), is a publicly available standard MRI dataset [2]. This dataset consists of 416 cross sectional data from subjects aged between 18 and 96. The images in the dataset are of 1.25mm thickness and of $256 \times 256 \times 128$ resolution.

3.1.2. IBSR18

The Internet Brain Segmentation Repository (IBSR18) [3] was created by the Center for Morphometic Analysis at the Massachusetts General Hospital. IBSR18 contains 18 T1 weighted MR brain images and their corresponding segmentation ground truth images. The images have 1.55 mm thickness with a resolution of $256 \times 256 \times 128$. All the images are bias field corrected using the Autoseg method developed by the University of North Carolina at Chapel Hill [4].

3.2. Evaluation Metrics

Usually, the segmentation results are evaluated for CSF, GM, and WM tissues using the following three evaluation metrics: overlap measure, boundary measure and volume measure. In this paper, we evaluate our proposed method using all the three measures.

Dice similarity Coefficient (DC): Dice similarity coefficient [32] is used to estimate the spatial overlap between the ground truth and the segmentation results, using the following equation.

$$DC = \frac{2 * |Seg\_Im \cap GT\_Im|}{|Seg\_Im| + |GT\_Im|} \tag{27}$$

where Seg_Im is the segmentation result of the proposed method and GT_Im is the ground truth. Higher DC represents more accurate segmentation.

Hausdorff Distance (HD): The Hausdorff distance [33] is used as the boundary measure and it is calculated between the ground truth points φ and the segmented points $\hat{\varphi}$ using the following equation:

$$HD = \max_{\hat{\varphi} \in Seg\_Im} \min_{\varphi \in GT\_Im} |\hat{\varphi} - \varphi| \tag{28}$$

The original Hausdorff Distance is affected by outliers [34]. Thus, to reduce the influence of outliers we used the 95^{th} percentile of the Hausdorff distance. In the following therefore HD refers the 95^{th} percentile of the Hausdorff distance, and lower HD represents a more accurate result.

[2] See the "Open Access Series of Imaging Studies" (OASIS) project's web site athttps://www.oasis-brains.org/.
[3] See the "Internet Brain Segmentation Repository" (IBSR) project's web site athttps://https://www.nitrc.org/projects/ibsr/.
[4] See the "AutoSeg" repository https://https://https://www.nitrc.org/projects/autoseg/.

Preprints (www.preprints.org) | NOT PEER-REVIEWED | Posted: 26 April 2022 doi:10.20944/preprints202204.0244.v1

Absolute Volume Difference (AVD): Absolute Volume Difference is a volume measure used to compute volume difference between the ground truth and the obtained results. It is computed as follows:

$$AVD = \frac{|Seg\_Im| - |GT\_Im|}{|GT\_Im|} \tag{29}$$

Lower AVD indicates a more accurate segmentation.

3.3. Experimental Setup

In this paper, we set fuzzifier m value as 2, stopping criterion ε to 0.0001 and initialized cluster centers randomly. We used voxel intensity as a feature. We let the window size N_k vary in $\{3, 5, 7\}$. From the experiments, it is found that when $K = 3$, performance is better. Therefore we set K=3 in all the experiments. Also, in order to set the value of α, we varied α from 0.1 to 1. From the experiments, it is found that when $\alpha = 0.9$ performance is better, and this value was used in all the experiments. The proposed model is implemented and experimented in MatLab 2016a.

3.4. Results

3.4.1. Results on OASIS Dataset

The OASIS dataset contains the images which are already skull stripped. Bias field correction is done using the ROBEX tool [31]. Figure 1 shows the qualitative segmentation results obtained using proposed method. We compared the results of the proposed method with the seven state of the art methods. The comparison of their results are presented in Table 1. We notice that the proposed model has better performance with regard to CSF, GM and WM when compared to the other methods.

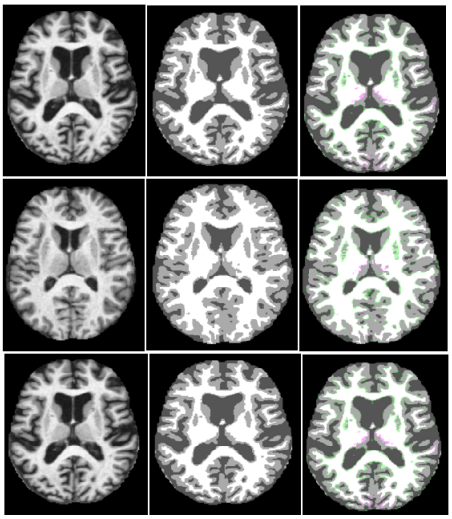

Figure 1. Segmentation results on OASIS dataset: first column original image, second column Ground Truth and third column segmentation result fused on ground truth

3.4.2. Results on IBSR18 Dataset

The images in the IBSR18 are already bias field corrected. Hence, we have not applied any bias field correction technique. We conducted the experiments by removing the skull using ground truth mask. Figure 2 shows the qualitative segmentation results obtained using proposed method. Table 2 presents the result comparison of proposed method and four individual clustering methods. The main limitation of the IBSR18 dataset is that it considers sulcal CSF as GM. [37] compared ten existing methods without considering the sulcal CSF. Following [38] and [39], in our study we did not removed the sulcal CSF. We have compared the results of the proposed method with state of art methods. As all the

Preprints (www.preprints.org) | NOT PEER-REVIEWED | Posted: 26 April 2022 doi:10.20944/preprints202204.0244.v1

Table 1. Results comparison with state of the art methods on OASIS dataset

Method	CSF			GM			WM		
	DC	HD	AVD	DC	HD	AVD	DC	HD	AVD
HMRF-EM [5]	61.47	7.17	12.51	79.65	5.14	4.11	83.82	5.09	3.33
FAST-PVE [35]	54.08	7.17	12.51	78.97	5.14	4.11	85.11	5.09	3.33
MSSEG [36]	89.95	4.18	4.71	91.24	4.31	2.87	89.58	4.39	2.91
RSKFCM [25]	90.06	4.06	4.31	92.31	4.21	2.31	90.51	4.31	2.81
GSKFCM [26]	91.23	4.08	4.28	92.51	4.13	2.11	90.62	4.28	2.71
MIFCM_S [17]	89.21	4.23	4.51	89.81	4.41	2.97	87.28	4.59	3.01
MIFCM_Y [17]	92.65	3.96	3.91	93.64	4.23	2.16	92.61	4.31	2.17
Proposed Method(consensus clustering)	**93.64**	**3.16**	**3.85**	**94.71**	**4.01**	**2.06**	**93.17**	**4.26**	**2.07**

considered methods have used DC alone as evaluation metric, Table 3 shows the results only on the DC of the IBSR18 dataset. From this comparison it is clear that the proposed model has better performance with regard to CSF, GM and WM when compared to the other methods.

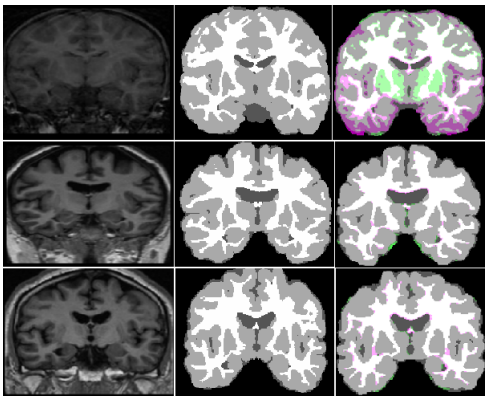

Figure 2. Segmentation results on IBSR18 dataset: first column original image, second column Ground Truth and third column segmentation result fused on ground truth

Table 2. Results on IBSR18 dataset

Method	CSF			GM			WM		
	DC	HD	AVD	DC	HD	AVD	DC	HD	AVD
RSKFCM[25]	93.41	5.02	5.26	93.55	5.16	3.59	96.68	4.98	3.40
GSKFCM [26]	93.43	4.96	5.25	93.58	5.08	3.52	96.72	4.96	3.38
MIFCM [17]	93.86	4.46	5.13	93.62	4.95	3.31	96.74	4.81	3.26
MIFCM [17]	94.02	4.02	5.01	93.64	4.91	3.21	96.82	4.78	3.06
Proposed Method (consensus clustering)	**95.68**	**3.91**	**4.74**	**94.50**	**4.32**	**2.93**	**97.31**	**4.67**	**2.91**

3.5. Discussion

On the OASIS dataset, the proposed method outperforms other methods in comparison. The OASIS dataset contains skull stripped T1 weighted MRI images. The main challenge in the OASIS dataset is the presence of WM lesion. The presence of WM lesion affects the overall segmentation accuracy of the proposed method. On the IBSR18 dataset, the proposed method outperforms all other methods in comparison. The images in IBSR18 dataset are affected by acquisition artifacts which have direct impact on the WM tissue segmentation. On the other hand, lack of sulcal CSF labelling in the ground truth affect the GM and the CSF tissue segmentation results.

In this paper, we have combined the results from four variants of FCM clustering methods. The RSKFCM and GSKFCM are proved to be less sensitive to noise due to use of kernel distance and addition of neighborhood information. The MIFCM_S and

 doi:10.20944/preprints202204.0244.v1

Table 3. Result comparison with state of the art methods on IBSR18 dataset only in terms of DC

Method	GM		WM		CSF	
	mean	std	mean	std	mean	std
R-FCM [40]	65.00	0.05	75.00	0.05	NA	NA
NL-FCM [40]	72.00	0.05	74.00	0.05	NA	NA
FCM [40]	74.00	0.05	72.00	0.05	NA	NA
HMRF-EM [5]	74.60	0.04	89.60	0.02	12.60	0.05
SFCM [41]	70.60	0.06	86.60	0.03	16.60	0.07
FANTASM [42]	71.60	0.06	88.60	0.03	11.60	0.06
PVC [28]	70.60	0.08	83.60	0.07	13.60	0.06
SPM5 [43]	68.60	0.07	86.60	0.02	10.60	0.05
GAMIXTURE [44]	78.60	0.08	87.60	0.02	15.60	0.09
ANN [45]	70.60	0.07	87.60	0.03	11.60	0.06
KNN [46]	79.60	0.03	86.60	0.03	16.60	0.07
BrainSuit09 [47]	72.00	0.09	83.00	0.08	NA	NA
SVPASEG [48]	81.60	0.03	88.60	0.02	16.60	0.07
SPM8 [49]	81.60	0.02	88.60	0.01	17.60	0.08
EGC-SOM [50]	73.00	0.05	76.00	0.04	NA	NA
HFS-SOM [50]	60.00	0.09	60.00	0.08	NA	NA
FAST-PVE [35]	78.00	0.08	86.00	0.04	NA	NA
FAST-PVE(S-ICM) [35]	78.00	0.08	86.00	0.04	NA	NA
RF-CRF [51]	96.10	0.01	92.00	0.02	92.00	0.03
RF-CRF1 [51]	94.00	0.01	89.00	0.02	88.00	0.03
RSKFCM [25]	96.68	0.09	93.55	0.10	93.41	0.08
GSKFCM [26]	96.72	0.03	93.58	0.02	93.43	0.02
MIFCM_S[17]	96.74	0.41	93.62	0.43	93.86	0.71
MIFCM_Y [17]	96.82	0.15	93.64	0.15	94.02	0.15
Proposed Method(consensus clustering)	**97.31**	**0.01**	**94.50**	**0.04**	**95.68**	**0.02**

MIFCM_Y are based on intutionistic fuzzy set which considers non membership value along with membership value. Thus, in comparison to RSKFCM and GSKFCM, MIFCM methods handled the uncertainty better and achieved better results. Since we combined the advantages of all four clustering methods, our proposed consensus clustering method achieved better results compared to individual clustering methods.

4. Conclusion

In this paper a new approach for MRI Brain tissue segmentation is presented. The proposed method is based on consensus clustering method. In consensus clustering the results of four variants of fuzzy clustering methods are combined to achieve better results. The results of the proposed methods are evaluated using three performance metrics i.e DC, HD and AVD. The competence of the proposed method is validated using three publicly available dataset: OASIS, IBSR18. From experimentation it has turned out that our proposed method obtains the best result compared to other contemporary methods on OASIS and IBSR18 dataset.

References

1. Despotovic, I.; Goossens, B.; Philips, W. MRI segmentation of the human brain: challenges, methods, and applications. *Computational and Mathematical Methods in Medicine* **2015**.
2. Coleman, G.B.; Andrews, H.C. Image segmentation by clustering. *Proceedings of the IEEE* **1979**, *67*, 773–785.
3. Chen, C.W.; Luo, J.; Parker, K.J. Image segmentation via adaptive K-mean clustering and knowledge-based morphological operations with biomedical applications. *IEEE Transactions on Image Processing* **1998**, *7*, 1673–1683.

4. Wu, M.N.; Lin, C.C.; Chang, C.C. Brain tumor detection using color-based k-means clustering segmentation. Third International Conference on Intelligent Information Hiding and Multimedia Signal Processing (IIHMSP). IEEE, 2007, Vol. 2, pp. 245–250.
5. Zhang, Y.; Brady, M.; Smith, S. Segmentation of brain MR images through a hidden Markov random field model and the expectation-maximization algorithm. *IEEE Transactions on Medical Imaging* **2001**, *20*, 45–57.
6. Phillips, W.; Velthuizen, R.; Phuphanich, S.; Hall, L.; Clarke, L.; Silbiger, M. Application of fuzzy c-means segmentation technique for tissue differentiation in MR images of a hemorrhagic glioblastoma multiforme. *Magnetic Resonance Imaging* **1995**, *13*, 277–290.
7. Kong, J.; Wang, J.; Lu, Y.; Zhang, J.; Li, Y.; Zhang, B. A novel approach for segmentation of MRI brain images. IEEE Mediterranean Electrotechnical Conference (MELECON), 2006, pp. 525–528.
8. Ahmed, M.N.; Yamany, S.M.; Mohamed, N.; Farag, A.A.; Moriarty, T. A modified fuzzy c-means algorithm for bias field estimation and segmentation of MRI data. *IEEE Transactions on Medical Imaging* **2002**, *21*, 193–199.
9. Liew, A.W.C.; Yan, H. An adaptive spatial fuzzy clustering algorithm for 3-D MR image segmentation. *IEEE Transactions on Medical Imaging* **2003**, *22*, 1063–1075.
10. Wang, J.; Kong, J.; Lu, Y.; Qi, M.; Zhang, B. A modified FCM algorithm for MRI brain image segmentation using both local and non-local spatial constraints. *Computerized Medical Imaging and Graphics* **2008**, *32*, 685–698.
11. Zhang, D.Q.; Chen, S.C. Clustering incomplete data using kernel-based fuzzy c-means algorithm. *Neural processing letters* **2003**, *18*, 155–162.
12. Lin, K.P. A novel evolutionary kernel intuitionistic fuzzy *c*-means clustering algorithm. *IEEE Transactions on Fuzzy systems* **2014**, *22*, 1074–1087.
13. Atanassov, K.T. Intuitionistic fuzzy sets. *Fuzzy sets and Systems* **1986**, *20*, 87–96.
14. Iakovidis, D.K.; Pelekis, N.; Kotsifakos, E.; Kopanakis, I. Intuitionistic fuzzy clustering with applications in computer vision. International Conference on Advanced Concepts for Intelligent Vision Systems. Springer, 2008, pp. 764–774.
15. Chaira, T. A novel intuitionistic fuzzy C means clustering algorithm and its application to medical images. *Applied Soft Computing* **2011**, *11*, 1711–1717.
16. Kumar, S.A.; Harish, B.; Aradhya, V.M. A picture fuzzy clustering approach for brain tumor segmentation. Cognitive Computing and Information Processing (CCIP), 2016 Second International Conference on. IEEE, 2016, pp. 1–6.
17. Kumar, S.A.; Harish, B. A Modified intuitionistic fuzzy clustering algorithm for medical image segmentation. *Journal of Intelligent Systems* **2017**.
18. Verma, H.; Agrawal, R.; Sharan, A. An improved intuitionistic fuzzy c-means clustering algorithm incorporating local information for brain image segmentation. *Applied Soft Computing* **2016**, *46*, 543–557.
19. Pedrycz, W.; Rai, P. Collaborative clustering with the use of Fuzzy C-Means and its quantification. *Fuzzy Sets and Systems* **2008**, *159*, 2399–2427.
20. Punera, K.; Ghosh, J. Consensus-based ensembles of soft clusterings. *Applied Artificial Intelligence* **2008**, *22*, 780–810.
21. Sevillano, X.; Alías, F.; Socoró, J.C. BordaConsensus: a new consensus function for soft cluster ensembles. Proceedings of the 30th annual international ACM SIGIR conference on Research and development in information retrieval. ACM, 2007, pp. 743–744.
22. Crespo, F.; Weber, R. A methodology for dynamic data mining based on fuzzy clustering. *Fuzzy Sets and Systems* **2005**, *150*, 267–284.
23. Pedrycz, W. A dynamic data granulation through adjustable fuzzy clustering. *Pattern Recognition Letters* **2008**, *29*, 2059–2066.
24. Wu, J.; Wu, Z.; Cao, J.; Liu, H.; Chen, G.; Zhang, Y. Fuzzy Consensus Clustering With Applications on Big Data. *IEEE Transactions on Fuzzy Systems* **2017**, *25*, 1430–1445.
25. Kumar, S.A.; Harish, B. Segmenting mri brain images using novel robust spatial kernel fcm (rskfcm). Eighth International Conference on Image and Signal Processing, 2014, pp. 38–44.
26. Kumar, S.A.; Harish, B.; Shivakumara, P. A novel fuzzy clustering based system for medical image segmentation. *International Journal of Computational Intelligence Studies* **2018**, *7*, 33–66.
27. Smith, S.M. Fast robust automated brain extraction. *Human brain mapping* **2002**, *17*, 143–155.
28. Shattuck, D.W.; Sandor-Leahy, S.R.; Schaper, K.A.; Rottenberg, D.A.; Leahy, R.M. Magnetic resonance image tissue classification using a partial volume model. *NeuroImage* **2001**, *13*, 856–876.

29. Mikheev, A.; Nevsky, G.; Govindan, S.; Grossman, R.; Rusinek, H. Fully automatic segmentation of the brain from T1-weighted MRI using Bridge Burner algorithm. *Journal of Magnetic Resonance Imaging* **2008**, *27*, 1235–1241.
30. Sadananthan, S.A.; Zheng, W.; Chee, M.W.; Zagorodnov, V. Skull stripping using graph cuts. *NeuroImage* **2010**, *49*, 225–239.
31. Iglesias, J.E.; Liu, C.Y.; Thompson, P.M.; Tu, Z. Robust brain extraction across datasets and comparison with publicly available methods. *IEEE Transactions on Medical Imaging* **2011**, *30*, 1617–1634.
32. Dice, L.R. Measures of the amount of ecologic association between species. *Ecology* **1945**, *26*, 297–302.
33. Huttenlocher, D.P.; Klanderman, G.A.; Rucklidge, W.J. Comparing images using the Hausdorff distance. *IEEE Transactions on Pattern Analysis and Machine Intelligence* **1993**, *15*, 850–863.
34. Mendrik, A.M.; Vincken, K.L.; Kuijf, H.J.; Breeuwer, M.; Bouvy, W.H.; De Bresser, J.; Alansary, A.; De Bruijne, M.; Carass, A.; El-Baz, A.; et al. MRBrainS challenge: online evaluation framework for brain image segmentation in 3T MRI scans. *Computational intelligence and neuroscience* **2015**, *2015*, 1.
35. Tohka, J. FAST-PVE: Extremely fast Markov random field based brain MRI tissue classification. Scandinavian Conference on Image Analysis. Springer, 2013, pp. 266–276.
36. Valverde, S.; Oliver, A.; Roura, E.; González-Villà, S.; Pareto, D.; Vilanova, J.C.; Ramio-Torrenta, L.; Rovira, A.; Llado, X. Automated tissue segmentation of MR brain images in the presence of white matter lesions. *Medical Image Analysis* **2017**, *35*, 446–457.
37. Valverde, S.; Oliver, A.; Cabezas, M.; Roura, E.; Llado, X. Comparison of 10 brain tissue segmentation methods using revisited IBSR annotations. *Journal of Magnetic Resonance Imaging* **2015**, *41*, 93–101.
38. Yi, Z.; Criminisi, A.; Shotton, J.; Blake, A. Discriminative, semantic segmentation of brain tissue in MR images. *Medical Image Computing and Computer-Assisted Intervention–MICCAI* **2009**, pp. 558–565.
39. Yaqub, M.; Javaid, M.K.; Cooper, C.; Noble, J.A. Investigation of the role of feature selection and weighted voting in random forests for 3-D volumetric segmentation. *IEEE Transactions on Medical Imaging* **2014**, *33*, 258–271.
40. Pham, D.L.; Prince, J.L. Adaptive fuzzy segmentation of magnetic resonance images. *IEEE Transactions on Medical Imaging* **1999**, *18*, 737–752.
41. Pham, D.L. Spatial models for fuzzy clustering. *Computer vision and image understanding* **2001**, *84*, 285–297.
42. Pham, D.L. Robust fuzzy segmentation of magnetic resonance images. Proceedings. 14th IEEE Symposium on Computer-Based Medical Systems (CBMS), 2001, pp. 127–131.
43. Ashburner, J.; Friston, K.J. Unified segmentation. *Neuroimage* **2005**, *26*, 839–851.
44. Tohka, J.; Krestyannikov, E.; Dinov, I.D.; Graham, A.M.; Shattuck, D.W.; Ruotsalainen, U.; Toga, A.W. Genetic algorithms for finite mixture model based voxel classification in neuroimaging. *IEEE Transactions on Medical Imaging* **2007**, *26*, 696–711.
45. Tian, D.; Fan, L. A brain MR images segmentation method based on SOM neural network. The 1st IEEE International Conference on Bioinformatics and Biomedical Engineering (ICBBE), 2007, pp. 686–689.
46. De Boer, R.; Vrooman, H.A.; Van Der Lijn, F.; Vernooij, M.W.; Ikram, M.A.; Van Der Lugt, A.; Breteler, M.M.; Niessen, W.J. White matter lesion extension to automatic brain tissue segmentation on MRI. *Neuroimage* **2009**, *45*, 1151–1161.
47. Shattuc, D.; Leahy, R. BrainSuite: an automated cortical surface identification tool. *Med Image Anal* **2002**, *6*, 129–142.
48. Tohka, J.; Dinov, I.D.; Shattuck, D.W.; Toga, A.W. Brain MRI tissue classification based on local Markov random fields. *Magnetic Resonance Imaging* **2010**, *28*, 557–573.
49. Ashburner, J.; Barnes, G.; Chen, C.; Daunizeau, J.; Flandin, G.; Friston, K.; Kiebel, S.; Kilner, J.; Litvak, V.; Moran, R. SPM8 Manual. Wellcome Trust Centre for Neuroimaging Institute of Neurology, UCL, 2012.
50. Ortiz, A.; Gorriz, J.; Ramirez, J.; Salas-Gonzalez, D.; Llamas-Elvira, J.M. Two fully-unsupervised methods for MR brain image segmentation using SOM-based strategies. *Applied Soft Computing* **2013**, *13*, 2668–2682.
51. Pereira, S.; Pinto, A.; Oliveira, J.; Mendrik, A.M.; Correia, J.H.; Silva, C.A. Automatic brain tissue segmentation in MR images using Random Forests and Conditional Random Fields. *Journal of Neuroscience Methods* **2016**, *270*, 111–123.